Synthesis of PPy- Nd_2O_3 nano-composite for utilization in supercapacitor applications

F. J. Hameed[a,*], I. M. Ibrahim[b*]
[a]*Department of Physics, College of Science, University of Baghdad, Baghdad, Iraq*
[b]*University of Baghdad, College of Science, Department of Physics, Baghdad, Iraq*

In this study, chemical oxidation was employed for the synthesis of polypyrrole (PPy) nanofiber. Furthermore, PPy has been subjected to treatment using nanoparticles of neodymium oxide (Nd_2O_3), which were produced and added in a certain ratio. The inquiry centered on the structural characteristics of the blend of polypyrrole and neodymium oxide after their combination. The investigation utilises X-ray diffraction (XRD), FTIR, and Field Emission Scanning Electron Microscopy (FE-SEM) for PPy, 10%, 30%, and 50% by volume of Nd_2O_3. According to the electrochemical tests, it has been noted that the nanocomposites exhibit a substantial amount of pseudocapacitive activity.

(Received May 22, 2024; Accepted August 5, 2024)

Keywords: Polypyrrole (PPy), Structural properties, Supercapacitor, Capacitance

1. Introduction

Conducting polymers (CPs) may effectively carry the charge current of an electron across the polymer network in electrochemical activities, given favorable conditions[1][2]. Due to their significant surface area to volume ratio, extended length, uniform diameter, huge surface area, and low density, they can be utilized as templates [3], [4]. PPy is extensively utilized as a conductive polymer due to its convenient mixing properties, high conductivity, and environmental stability [5], [6]. Bonding is the primary prerequisite for PPy's electrical effects. By catalyzing the combination of various substances such as cations, inorganic anions, and natural molecules, it is expected that the electrical conductivity of PPy will be enhanced [7]. The unique characteristics of CPs offer novel possibilities for mechanical functions, such as the capacity to replenish batteries or generate biological sensitivities. CPs have the ability to store capacitance through the process of countercharge accumulation and release, which is caused by redox reactions taking place in an electric field [8]–[12]. Scientists worldwide continue to closely examine the implementation of electrostatic polymers. These conductive polymers have unique electrochemical characteristics that allow them to discharge and dope rapidly. The purpose of this method is to confine the charge within all volumes. Only a limited number of conductive polymers, such as polypyrrole (PPy), poly 1, 5-diamino anthraquinone, and polyaniline (PANI), demonstrate the property of super-condensation. PPy is a highly specialized polymer due to its exceptional conductivity, significant storage capacity, environmental resilience, and strong redox current [13]–[15]. Capacitors are commonly built by arranging a set of parallel plates that are separated by an insulating material. When a voltage is applied in series to the plates, the capacitive charge of the plates with opposite signs starts to accumulate. Supercapacitors possess a greater capacity (F) compared to normal capacitors[16], but they exhibit lower power values (mF). This work aimed to construct an electronic electrode, analyze its structural properties, and subsequently evaluate the supercapacitor using various techniques such as galvanostatic charge-discharge (GCD), electrochemical impedance spectroscopy (EIS) and cyclic voltammetry (CV) measurements.

* Corresponding authors: firasalhbolee@gmail.com
https://doi.org/10.15251/JOR.2024.204.525

2. Experimental investigation

2.1. Production of PPy nanofiber

The methodology proposed by Hameed and Ibrahim [17] was employed to fabricate the composite of polypyrrole nanostructure. In the initial phase, 0.818 g of methyl orange was uniformly distributed in 60 mL of distilled water. A solution containing 2.237 grams of ferric chloride was mixed with methyl orange under gentle stirring at a speed of 80 revolutions per minute. The mixture was then placed in an ice bath and 1 milliliter of pyrrole was added. The liquid turned black and was churned continuously for a duration of 24 hours. The precipitate was subjected to several washes using ethanol and distilled water, followed by filtration and drying for a duration of 60 minutes.

2.2. Preparation of PPy-Nd2O3 nanocomposite

It involves the combination of polypyrrole (PPy) with neodymium oxide (Nd_2O_3). In order to produce a uniform and readily usable mixture, an appropriate quantity of neodymium oxide (Nd_2O_3) was dissolved in distilled water. This solution was then added to polypyrrole (PPy) at volume ratios of 10%, 30%, and 50%. The resulting mixture was subjected to ultrasonic waves for a duration of one hour.

2.3. The electrode's fabrication process

The PPy- Nd_2O_3 electrode was fabricated on a nickel foam substrate measuring 1*1 cm^2. The technique of drop casting was employed to coat a nickel foam substrate with a PPy- Nd_2O_3 nanocomposite, with the compositions of 10%,30% and 50% correspondingly. The synthesized specimen (PPy- Nd_2O_3/nickel foam) underwent testing utilizing cyclic voltammetry (CV), galvanostatic charge-discharge analysis (GCD), and electrochemical impedance spectroscopy (EIS) in a 1 ml solution of concentrated sulphuric acid (100% H_2SO_4). The weight of the electrode (PPy-Nd_2O_3) was 0.7 mg. This method of preparing the electrode is identical to the reference [18].

3. Findings and analysis

3.1. Examining X-ray diffraction

Figure 1 depicts the X-ray diffraction patterns of a nanofiber of PPy, a nanoparticle of Nd_2O_3, and a nanocomposite of PPy- Nd_2O_3. This observation illustrates that the X-ray pattern of pure polypyrrole (PPy) exhibits a diffraction peak at $2\theta = 20.35$. Additionally, it shows a wide peak for 2θ values spanning from 13° to 29°. This peak has low intensity and a wide shape, providing evidence that the chemical under consideration is amorphous [19]. The presence of prominent diffraction peaks in Nd_2O_3 indicates that the material possesses a crystalline structure in its inherent condition. Perform X-ray diffraction (XRD) analysis on samples containing 10%, 30%, and 50% of Nd_2O_3. The diffraction peaks observed at 10.5 degrees, 14 degrees, 16.3 degrees, 28 degrees, 29.1 degrees, 32.4 degrees, 37.2 degrees, 40.8 degrees, 50 degrees and 57.4 degrees are found to be associated with the characteristic peaks of Nd_2O_3, specifically matching the code 1523969 in the Crystallography Open Database. The peaks observed in the data correspond to the crystal planes with Miller indices of (001), (100), (002), (011), (012), (003), (110), (111), (103) and (200), respectively. Based on the findings documented by [20], [21]. The data clearly shows that when the PPy- Nd_2O_3 nanocomposites contain 10%, 30%, and 50% of Nd_2O_3, there are only ten broad peaks observed for Nd_2O_3. On the other hand, the broad peak from PPy is observed with a much lower intensity. This suggests that during the polymerization reaction, the crystal structure of the Nd_2O_3 particles may become distorted and transition into an amorphous phase, In addition to the transformation of the cubic phase into a hexagonal phase which could explain this phenomenon [21], [22]. Figure 1 displays the X-ray diffraction (XRD) patterns of pure polypyrrole (PPy) and various proportions of the PPy- Nd_2O_3 composite.

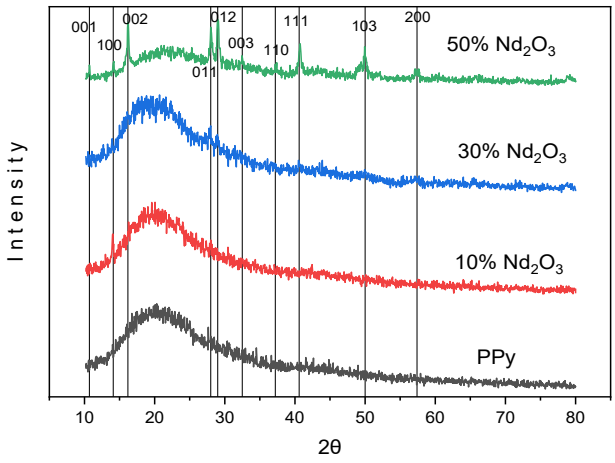

Fig. 1. Displays the X-ray diffraction (XRD) patterns of pure polypyrrole (PPy) and various proportions of the PPy- Nd_2O_3 composite.

3.2. Fourier transform infrared (FTIR) analysis

The manufacture of the polypyrrole-graphene oxide composite has been confirmed through the examination of FTIR spectra. Figure 2 displays the spectra of different materials, including PPy and PPy-Nd_2O_3, with variable proportions (10%, 30%, and 50% of Nd_2O_3). The signal observed at 1050 cm^{-1} corresponds to the O-H bending vibration of PPy, while the signal identified at 1090 cm^{-1} corresponds to the O-H bending vibration of PPy-Nd_2O_3 [23]. The signal recorded at 610 cm^{-1} and 660 cm^{-1} is attributed to the vibration of Nd-O bonds[24]. The peak observed at 1600 cm^{-1} and 3605 cm^{-1} is attributed to the stretching vibration of the -OH group [24], [25]. The PPy FTIR spectrum exhibits a peak at 3150 cm^{-1} and 890 cm^{-1}, which can be attributed to the C-H stretching vibration mode [26]. The PPy- Nd_2O_3 composite exhibited a shift of the peak at 1050 cm^{-1} in the PPy spectra to 1090 cm^{-1} in PPy-Nd_2O_3. This shift can be attributed to an interaction between PPy and Nd_2O_3, which impacts the O-H bending vibration of PPy-Nd_2O_3. The peaks observed at 1050 cm^{-1}, 1590 cm^{-1}, and 831 cm^{-1} in the PPy spectra have shifted to 1090 cm^{-1},1600 cm^{-1}, and 890 cm^{-1} in the PPy-Nd_2O_3 composite, respectively. This shift is attributed to the interaction between PPy and Nd_2O_3, which affects the Nd-O vibration, O-H bending vibration, stretching vibration of the -OH group, and C-H stretching vibration, as reported in references [23]–[26].

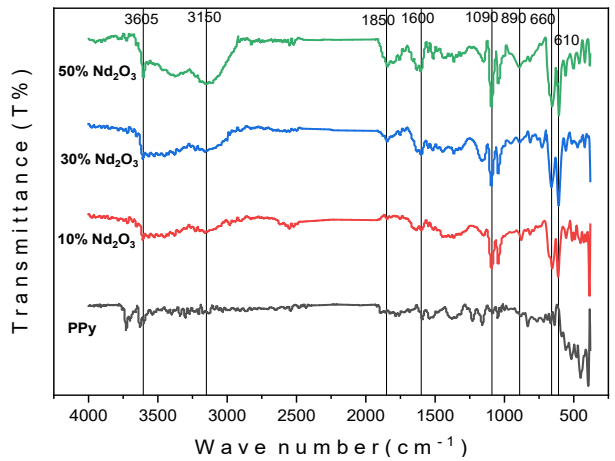

Fig. 2. FTIR of PPy, 10%, 30%, and 50% Nd_2O_3.

3.3. An examination of the field emission scanning electron microscope (FE-SEM*)*

The field emission scanning electron microscopy (FE-SEM) technique was used to evaluate the surface morphology of the as-made PPy and PPy-Nd_2O_3 hybrid nanocomposite films, as shown in Figure 3. The microstructure images depicted in Figures 3a and 3b exhibit the nanofiber structures of pure PPy at magnifications of 350000 X and 135000 X, respectively. PPy was produced utilizing the method of chemical oxidation and an ice bath, as previously stated. Upon morphological examination, it was observed from the photos that the material is composed of nanofibers. The morphology of the PPy- Nd_2O_3 nanocomposites is depicted in Figure 3a and Figure 3b, showing a consistent arrangement of PPy nanofibers and Nd_2O_3 nanoparticles. The images were taken at different magnifications (10%, 30%, and 50% Nd_2O_3). The majority of these nanofibers have sizes that range from 30 to 100 nm. The PPy- Nd_2O_3 hybrid nanocomposites display the occurrence and clustering of PPy fibers on the surface, resulting from the interactions between the fibers and Nd_2O_3 particles, as observed in the FESEM images. An attraction between PPy and Nd_2O_3 develops when particular quantities of Nd_2O_3 are introduced. Nevertheless, the introduction of substantial quantities of Nd_2O_3 will result in a stronger attraction between the Nd_2O_3 molecules and the PPy, causing the formation of tiny clusters on the PPy surface. The results of the photographs are nearly identical to those of the second study [27], [28].

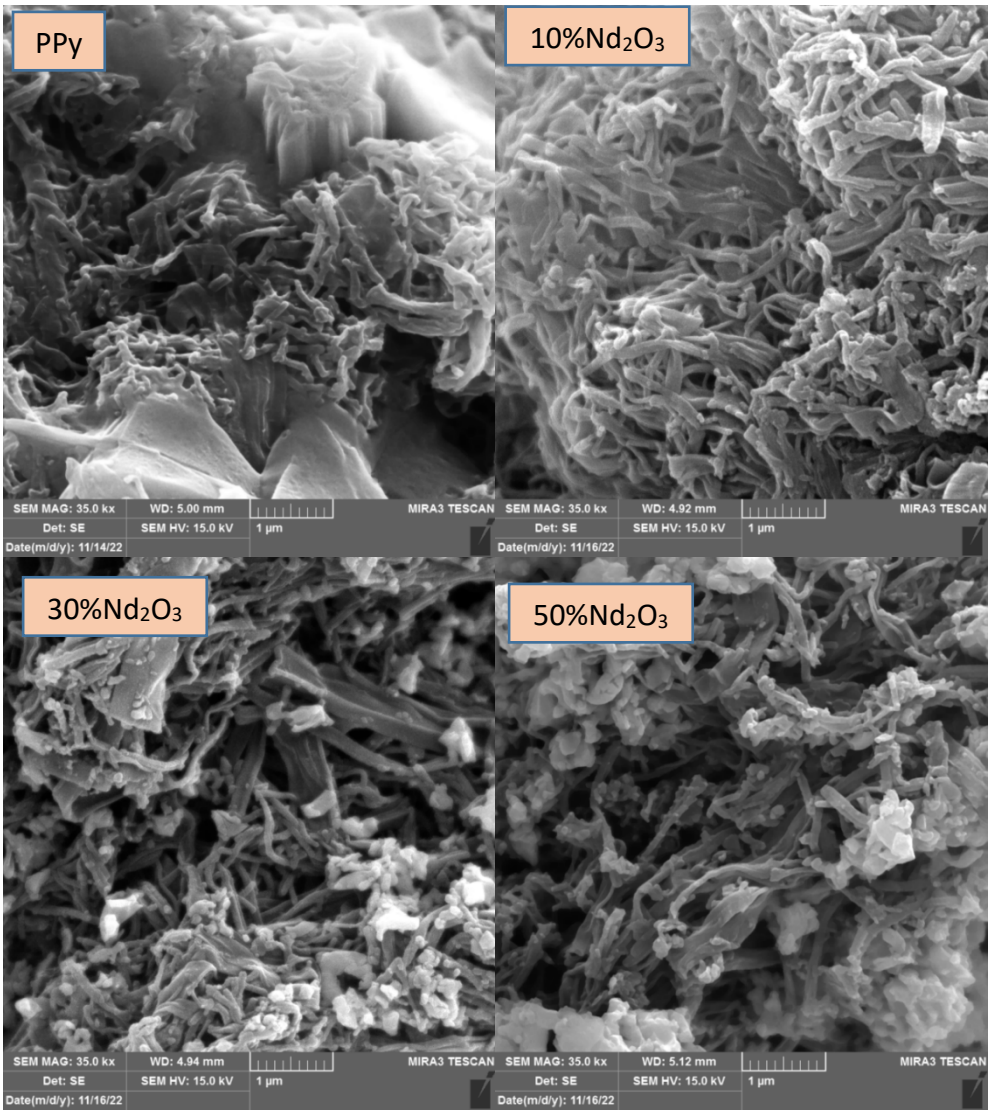

Fig. 3. a shows 35000-magnified FESEM images of PPy, 10% Nd_2O_3, 30% Nd_2O_3, and 50% Nd_2O_3.

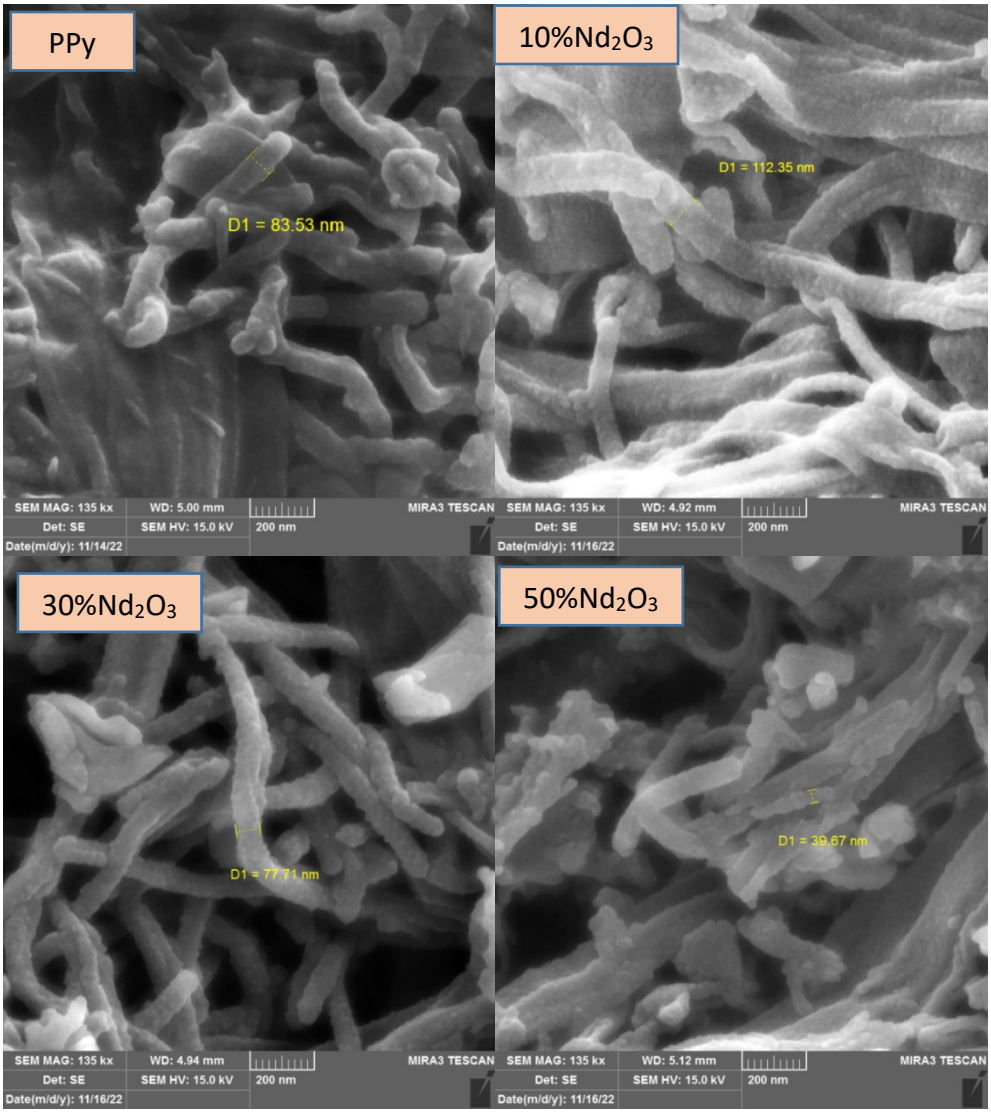

Fig. 3. b shows 135000-magnified FESEM images of PPy, 10% Nd_2O_3, 30% Nd_2O_3, and 50% Nd_2O_3.

3.4. Figure of merit of a supercapacitor

The initial evaluation of the electrochemical performance is conducted by systematically measuring it using cyclic voltammetry (CV), galvanostatic charge/discharge (GCD), and electrochemical impedance spectroscopy (EIS) in a conventional three-electrode configuration.

3.4.1. Cyclic voltammetry (CV)

Cyclic Voltammetry is a technique used to measure the current response of an electrochemical system as a function of the applied voltage, which is varied in a cyclic manner. Cyclic voltammetry is an effective electrochemical technique that can be utilized to ascertain the primary pathway of electron transfer over time and under varying applied potentials [29]. Figure 4 (A-C) illustrates the results of the cyclic voltammetry analysis performed on the PPy and PPy- Nd_2O_3 films. The anode and cathode peaks may be noticed at the following current values: (3.31, 5.05, 5.52, 4.87), (6.22, 12, 12.4, 11.2), and (13.4, 17.8, 18, 16.7) mA, respectively. These observations were made by repeatedly applying the scan rate values of (50, 100, 150) mV. The materials have electrochemical reactivity within a defined range of potential, as evidenced by the cyclic voltammetry (CV) data. CV curves display a distinct pair of redox peaks, which is a common property of battery-type electrodes [30]. The electrochemical characteristics of polypyrrole (PPy) and Neodymium oxide (Nd_2O_3) are merged in the PPy- Nd_2O_3 composite film. The PPy- Nd_2O_3 nanocomposite membrane demonstrates a noticeable electrochemical response at potentials lower

than 0.75 V, as illustrated in Figure 4. The anode electrode acts as the source of positive charges, while the cathode electrode acts as the reservoir for positive charge carriers in the PPy and PPy-Nd_2O_3 materials. This device functions continuously during the entire discharge procedure. During a cathodic voltaic (CV) reaction, the cathode side of the system undergoes a color change and turns black, while the anode side remains white. The presence of a Gaussian shape in Figure 4 indicates that the electrochemical interaction has a far greater impact on PPy- Nd_2O_3 composites compared to pure PPy.

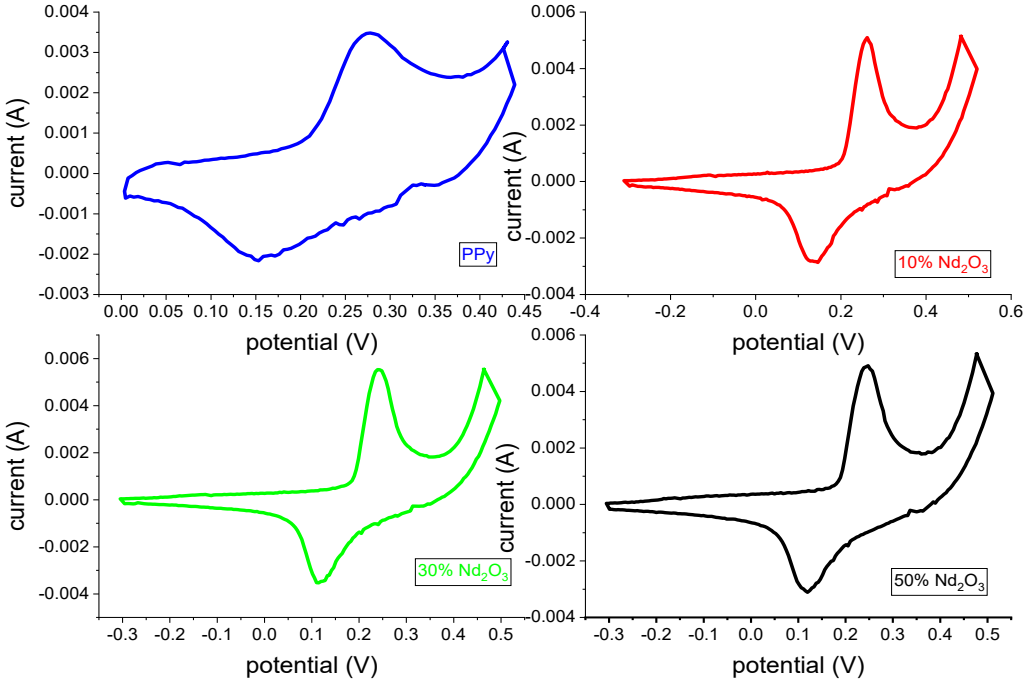

Fig. 4. A depicts the cyclic voltammetry of PPy and PPy- Nd_2O_3 nanocomposite at a voltage of 50 mV, with varying concentrations of Nd_2O_3.

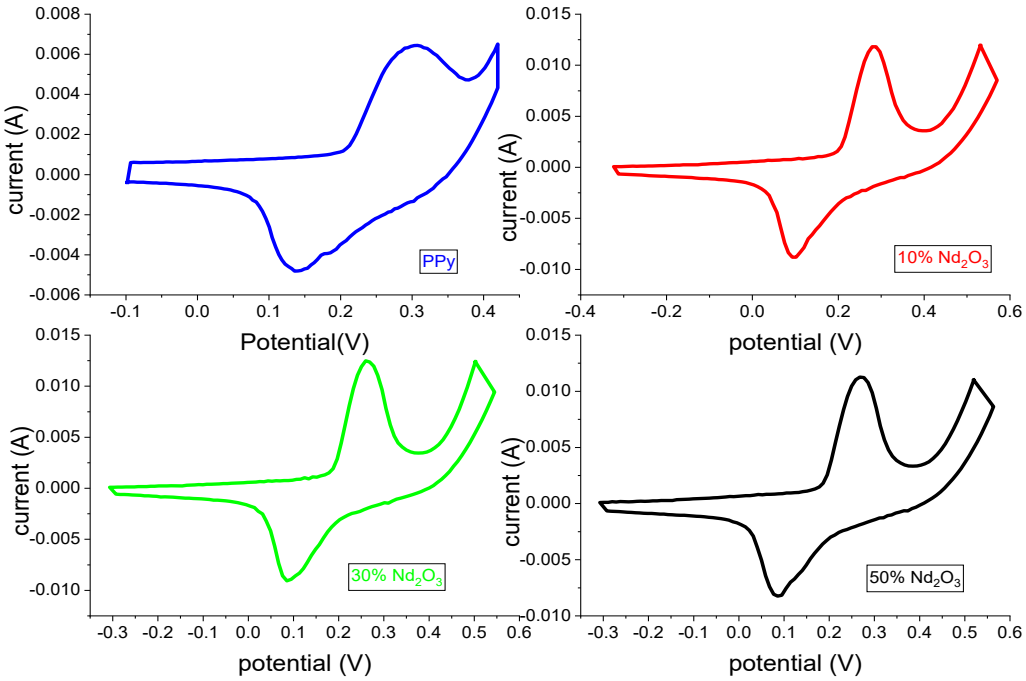

Fig. 4. B depicts the cyclic voltammetry of PPy and PPy- Nd_2O_3 nanocomposite at a voltage of 100 mV,

with varying concentrations of Nd_2O_3.

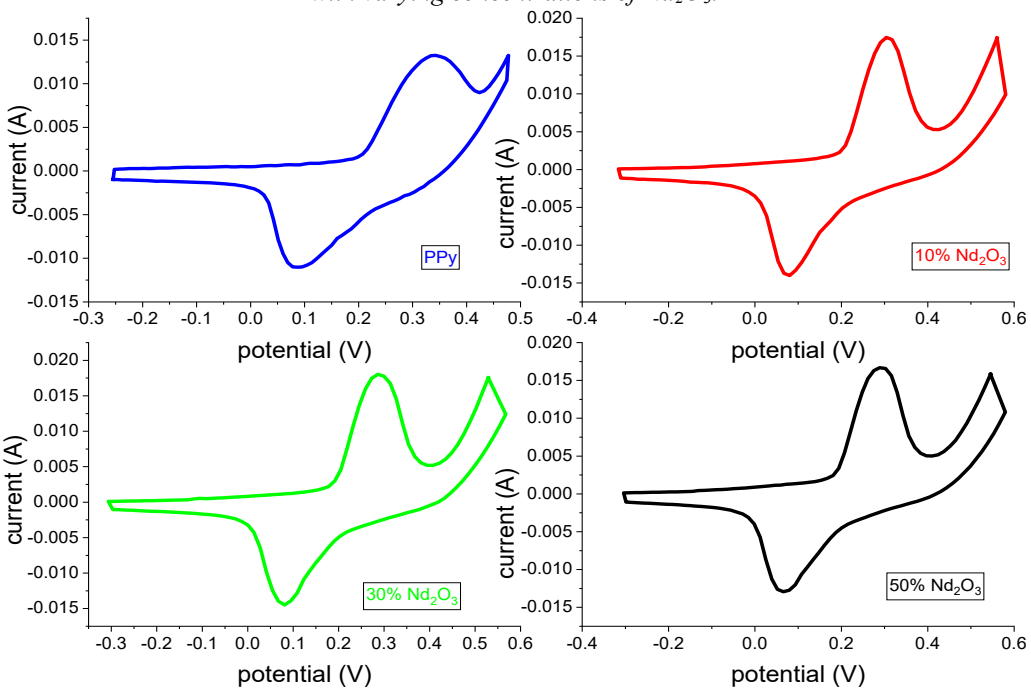

Fig. 4. C depicts the cyclic voltammetry of PPy and PPy- Nd_2O_3 nanocomposite at a voltage of 150 mV, with varying concentrations of Nd_2O_3.

The clarification might be achieved by using the synergistic effects of PPy and Nd_2O_3. The appearance of two clearly defined and significant redox peaks on each curve shown in Figure 4 (A-C) suggests the existence of a pseudo-capacitative characteristic in the supercapacitor. This characteristic arises from the Faradaic redox processes. The PPy- Nd_2O_3 composite membrane exhibited comparable characteristics to those documented in references [31], [32]. Commercial SuperCapacitors often prefer organic electrolytes due to their wide voltage ranges and high energy density. However, aqueous electrolytes are a cost-effective alternative that may be easily handled in a laboratory setting without any specific conditions.

3.4.2. Galvanostatic charge-discharge (GCD)

A galvanostatic charge/discharge test [17] was used to evaluate the electrochemical performance of the hybrid PPy- Nd_2O_3 electrode. To achieve the best possible performance of the hybrid system, the variations of different electrodes were evaluated separately when a Ni-foam reference anode was added [33]. The purpose of this was to ascertain the optimal operational range with the greatest impact [34]. The potential variations in the negative and positive electrodes are almost inclined, with one and two phases correspondingly. These fluctuations arise throughout the process of charging and discharging and bear resemblance to the constant voltage (CV) information depicted in Figure 4. This outcome is a consequence of the possible interconnectedness of redox reactions. PPy, a polymer with the ability to incorporate anions, suffers p-doping. A polaron is created when the ongoing movement of electrons from a neutral part of their quinoid chains causes a localised change in positive charge [35]. Both the PPy and the PPy- Nd_2O_3 electrodes exhibit efficient performance within the standard potential ranges throughout the charge/discharge processes (Fig. 5). Furthermore, the PPy- Nd_2O_3 hybrid composite electrode demonstrates the capability to function within a specific range of electrical potential, specifically 0.2 V [34]. The specific capacitance can be calculated by utilising the CD curve and applying the equation [36]. The specific capacitance (C) is determined by the following equation:

$$C = I * \Delta t / \Delta V * m \quad (1)$$

In this equation, C is measured in Farads per gramme (F. g^{-1}), ΔV represents the potential window in Volts (V) (specifically, 0.2 V), I is the discharge current in Amperes (A) (in this case, 0.5 mA), Δt is the discharge time in seconds (3.24 s for pure PPy, 5.19 s for 10% Nd_2O_3, 5.29 s for 30% Nd_2O_3, 3.86 s for 50% Nd_2O_3), and m is the mass of the electrode in grammes (PPy or PPy-Nd_2O_3, in this case it is 0.08 mg). By adding 10% Nd_2O_3, we increased the capacity of pure PPy from 101.25 (F.g^{-1}) to 162.18 (F.g^{-1}). In addition, by using up to 30% Nd_2O_3, we were able to further enhance the capacity to 165.31 (F.g^{-1}). Nevertheless, as the Nd_2O_3 level reached 50%, the capacity experienced a fall to 120.62 (F.g^{-1}). The observed behaviour can be ascribed to the electrostatic attraction between polypyrrol nanofibers and neodymium oxide, resulting in an augmentation of the surface area and, consequently, the capacitance [32]. The highest capacity value of 165.31 (F/g) was attained by the oxidative polymerization process in PPy- Nd_2O_3 nanocomposites and 1 M H_2SO_4 electrolysis.

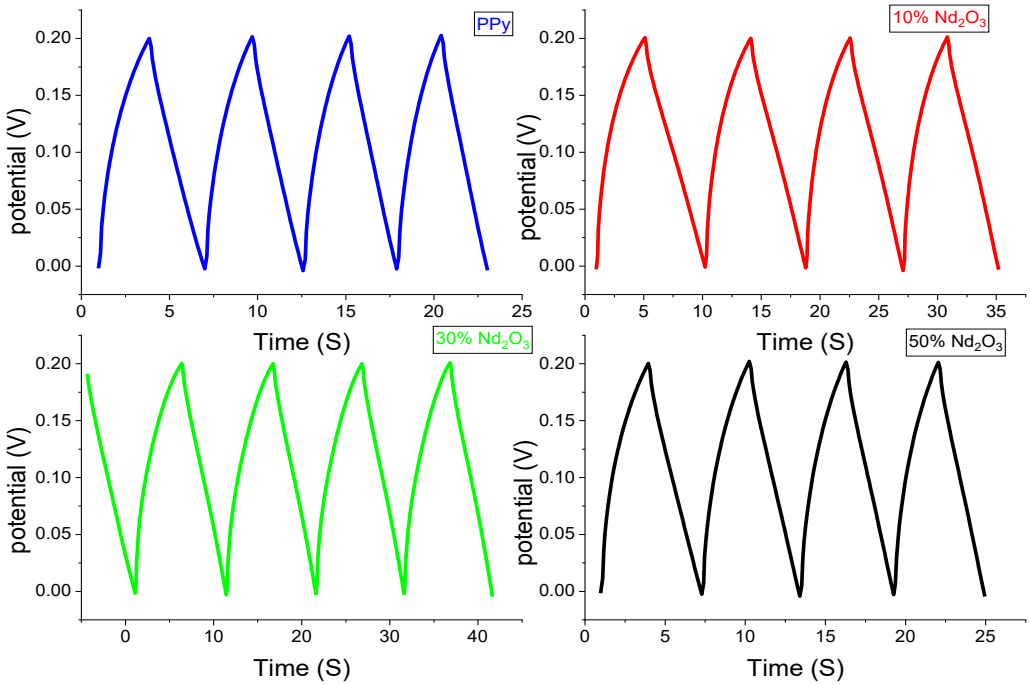

Fig. 5. Illustrates the galvanostatic charge-discharge behaviour of pure PPy and PPy- Nd_2O_3 at different percentages.

3.4.3. Electrochemical Impedance Spectroscopy (EIS)

The Nyquist plot was generated by applying a 5 mV AC voltage with an amplitude and frequency range of 1 Hz to 1000 kHz, respectively, at the open circuit potential. For additional information, please consult Figure 6. An electrochemical impedance spectroscopy (EIS) plot was performed on both PPy samples and PPy-Nd_2O_3 composites (Fig. 6) to understand the charge transfer of the PPy-Nd_2O_3 electrode material. The ohmic resistance can be measured by measuring the real component of the impedance at the point where the semicircle intersects with the high frequency. At higher frequencies, the tight semi-circle represents a low transfer resistance of the charge, while at lower frequencies there is a minor diffusion. A 45-degree slope in the low frequency domain of the beeline suggests that the process is governed by diffusion. In contrast, a slope of 90 degrees signifies a complete capacitive behaviour. The impedance map displays a semi-circular pattern, indicating a very efficient passage of electric charge. This finding offers additional proof to substantiate the remarkable resilience of the PPy-Nd_2O_3 nanocomposite throughout the process of electrochemical cycling. This material has shown promising potential as an electrode in electrochemical supercapacitors, as indicated by previous studies [32], [37].

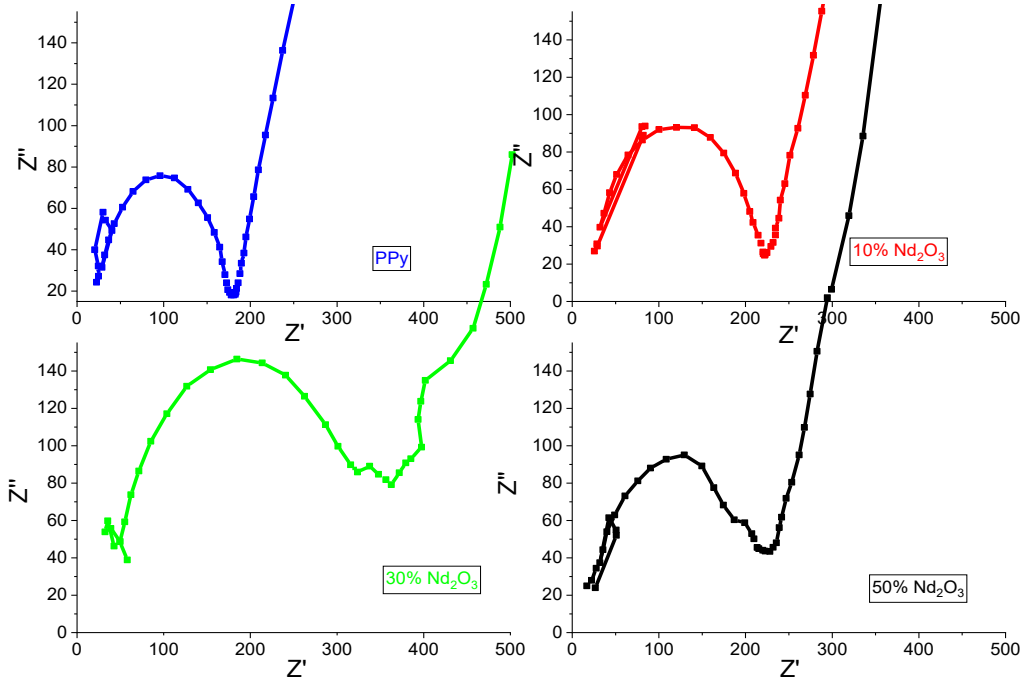

Fig. 6. Displays the Nyquist curves were obtained from electrochemical impedance spectroscopy tests conducted on the PPy and PPy-Nd_2O_3 samples.

4. Conclusion

In summary, PPy nanofiber and a nanocomposite of PPy-Nd_2O_3 have been synthesised utilising a simple method. The composite film consisting of PPy and Nd_2O_3 is an exceptional material for the electrode in electrochemical supercapacitors. The GCD curves demonstrated that PPy nanofibers, when doped with 30% Nd_2O_3, had the highest capacitance values, reaching 165.31 ($F.g^{-1}$). Nevertheless, the capacitance of pure PPy was much reduced in comparison to PPy doped with Nd_2O_3. Therefore, doping greatly increases the capacitance of supercapacitors.

References

[1] K. Dutta, S. Das, D. Rana, P. P. Kundu, Polymer Reviews 55(1), 1-56 (2015); https://doi.org/10.1080/15583724.2014.958771

[2] P. Santhosh, A. Gopalan, K.-P. Lee, Journal of Catalysis 238(1), 177-185 (2006); https://doi.org/10.1016/j.jcat.2005.12.014

[3] H. M. Hawy, I. M. Ali, Optik 262(April), 169263 (2022); https://doi.org/10.1016/j.ijleo.2022.169263

[4] A. J. Almusawe, T. F. Hassen, M. A. Rahma, N. F. Abd Alrasheed, Iraqi Journal of Science 59(1), 299-306 (2018).

[5] N. Yasser, N. A. Ali, L. H. Sulaiman, Iraqi Journal of Science 59 (1B), 294-298 (2018).

[6] M. A. Salman, S. M. Hassan, Iraqi Journal of Physics 19(48), 33-43 (2021); https://doi.org/10.30723/ijp.v19i48.614

[7] Z. Huang, P.-C. Wang, A. G. MacDiarmid, Y. Xia, G. Whitesides, Langmuir 13(24), 6480-6484 (1997); https://doi.org/10.1021/la970537z

[8] J. Jang, in Emissive Materials Nanomaterials 199(1), 189-260 (2006); https://doi.org/10.1007/12_075

[9] A. Babakhanian, S. Kaki, M. Ahmadi, H. Ehzari, A. Pashabadi, Biosensors and Bioelectronics 60(1), 185-190 (2014); https://doi.org/10.1016/j.bios.2014.03.058
[10] P. Novák, K. Müller, K. S. V Santhanam, O. Haas, Chemical Reviews 97(1), 207-282 (1997); https://doi.org/10.1021/cr941181o
[11] X. Lu, Y.Li, J.Du, X.Zhou, Z.Xue, X.Liu, Z.Wang, Electrochimica Acta 56(21), 7261-7266 (2011); https://doi.org/10.1016/j.electacta.2011.06.056
[12] Y.-Z. Long, M.-M.Li, C.Gu, M.Wan, J.-L.D, Z.Liu, Z.Fan, Progress in Polymer Science 36(10), 1415-1442 (2011); https://doi.org/10.1016/j.progpolymsci.2011.04.001
[13] P. Li, Y.Yang, E.Shi, Q.Shen, Y.Shang, S.Wu, J.Wei, K.Wang, H.Zhu, Q.Yang, ACS Applied Materials & Interfaces 6(7), 5228-5234 (2014); https://doi.org/10.1021/am500579c
[14] Q. Zhang, X. Zhou, H. Yang, Journal of Power Sources 125(1), 141-147 (2004); https://doi.org/10.1016/S0378-7753(03)00818-8
[15] Y. H. Park, K. W. Kim, W. H. Jo, Polymers for Advanced Technologies 13(9), 670-677 (2002); https://doi.org/10.1002/pat.331
[16] R. K. Sharma, A. C. Rastogi, S. B. Desu, Electrochimica Acta 53(26), 7690-7695 (2008); https://doi.org/10.1016/j.electacta.2008.04.028
[17] F. J. Hameed, I. M. Ibrahim, Iraqi Journal of Science 62(5), 1503-1512 (2021); https://doi.org/10.24996/ijs.2021.62.5.14
[18] V. Thennarasu and A. Prabakaran, Journal of Ovonic Research 19(5), 597–606 (2023); https://doi.org/10.15251/JOR.2023.195.597
[19] B. T. Raut, M. A. Chougule, A. A. Ghanwat, R. C. Pawar, C. S. Lee, V. B. Patil, Journal of Materials Science: Materials in Electronics 23(12), 2104-2109 (2012); https://doi.org/10.1007/s10854-012-0708-7
[20] P. Aldebert, J. P. Traverse, Materials Research Bulletin 14(3), 303-323 (1979); https://doi.org/10.1016/0025-5408(79)90095-3
[21] M. Shao, Y. Huang, J. Liu, X. Jia, K. An, L. Chen, J. Wei, C. Li, Vacuum 169 (September) 108936 (2019); https://doi.org/10.1016/j.vacuum.2019.108936
[22] M. D. Kannan, S. K. Narayandass, C. Balasubramanian, D. Mangalaraj, physica status solidi (a) 128(2), 427-433 (1991); https://doi.org/10.1002/pssa.2211280219
[23] Y. Song, M. Shang, J. Li, Y. Su, Chemical Engineering Journal 405(1), 127059 (2021); https://doi.org/10.1016/j.cej.2020.127059
[24] B. Umesh, B. Eraiah, H. Nagabhushana, B.M. Nagabhushana, G. Nagaraja, C. Shivakumara, R.P.S. Chakradhar, Journal of Alloys and Compounds 509(4), 1146-1151 (2011); https://doi.org/10.1016/j.jallcom.2010.09.143
[25] F. Liang, Z. Liu, Y. Liu, Journal of Materials Science: Materials in Electronics 28(1) 10603-10610 (2017); https://doi.org/10.1007/s10854-017-6835-4
[26] Y. Chen, X. Zhang, C. Xu, H. Xu, Electrochimica Acta 309(1), 424-431 (2019); https://doi.org/10.1016/j.electacta.2019.04.072
[27] T. Sreethawong, S. Chavadej, S. Ngamsinlapasathian, S. Yoshikawa, Solid State Sciences 10(1), 20-25 (2008); https://doi.org/10.1016/j.solidstatesciences.2007.08.010
[28] C. R. Michel, A. H. Martínez-Preciado, N. L. L. Contreras, Sensors and Actuators, B: Chemical 184(1), 8-14 (2013); https://doi.org/10.1016/j.snb.2013.04.044
[29] R. M. A. P. Lima H. P. de Oliveira, Journal of Energy Storage, 28(1), 101284, (2020); https://doi.org/10.1016/j.est.2020.101284
[30] W. He, G.Zhao, P.Sun, P.Hou, L.Zhu, T.Wang, L.Li, , X.Xu, T.Zhai, Nano Energy 56(1), 207-215 (2019); https://doi.org/10.1016/j.nanoen.2018.11.048
[31] E. Taer, A. Apriwandi, Y. S. Ningsih, R. Taslim, International Journal of Electrochemical Science 14(3), 2462-2475 (2019); https://doi.org/10.20964/2019.03.17
[32] F. Abdollahi, M. Shahidi-Zandi, M. M. Foroughi, M. Kazemipour, International Journal of Electrochemical Science 15(12), 11757-11768 (2020); https://doi.org/10.20964/2020.12.70

[33] K. D. Kumar, T. Ramachandran, Y. A. Kumar, A. A. A. Mohammed, M. Kang, Journal of Physics and Chemistry of Solids 185(1), 111735 (2024); https://doi.org/10.1016/j.jpcs.2023.111735

[34] B. Dahal, T.Mukhiya, G.P.Ojha, A.Muthurasu, S.-H.Chae, T.Kim, D.Kang, H.Y.Kim, Electrochimica Acta 301(1), (2019); https://doi.org/10.1016/j.electacta.2019.01.171

[35] T. Le, H. Yoon, Fundamentals of conjugated polymer nanostructures, Conjugated Polymer Nanostructures for Energy Conversion and Storage Applications 1-42 (2021); https://doi.org/10.1002/9783527820115.ch1

[36] A. P. Tiwari, S.-H.Chae, G. P.Ojha, B.Dahal, T.Mukhiya, M.Lee, K.Chhetri, T.Kim, H.-Y. Kim, Journal of colloid and interface science 553(1), 622-630 (2019); https://doi.org/10.1016/j.jcis.2019.06.070

[37] J. Tan, X.He, F.Yin, B.Chen, G.Li, X.Liang, H.Yin, Catalysis Today 364(December) 67-79 (2021); https://doi.org/10.1016/j.cattod.2019.12.018